

Application of back-propagation neural network on bank destruction forecasting for accumulative landslides in the three Gorges Reservoir Region, China

Changdong Li · Huiming Tang · Yunfeng Ge ·
Xinli Hu · Liangqing Wang

Published online: 22 January 2014
© Springer-Verlag Berlin Heidelberg 2014

Abstract In recent years, a large number of bank destruction occur in the reservoir area under the effect of water fluctuation, which may be lead to reservoir accumulative landslide geological hazards finally. The paper conducted the bank destruction forecasting study for accumulative landslides in the Three Gorges Reservoir Region, China utilizing back-propagation (BP) neural network approach. A representative scenario of Jinle landslide is then taken for analysis purposes. On the basis of the existing data sets of bank destruction cases, the BP neural network forecasting model and the corresponding programs for bank destruction are both presented, whose forecasting result is validated by two independent approaches, namely empirical method and numerical modeling method. Furthermore, the BP neural network model had obvious advantages over the convention approaches in the aspects of the fast calculation speed and high convenience. According to the bank destruction forecasting scale presented above, the corresponding revetment measures can be proposed to prevent the occurring of the bank destruction, whose effectiveness has been further validated by the actual engineering practice.

Keywords Accumulative landslide · Bank destruction forecasting · BP neural network · Numerical modelling

1 Introduction

With the fast development of human activities, there are more and more geological hazards occurring all over the world, which are intensively interested by a great number of scholars in the geological hazard field. Some of the causes of geological hazards, such as landslide and bank destruction, are related to geo-hydrological hazards; as a result, people began to realize the significant role of groundwater and surface water to the stability of landslide. The Three Gorges Reservoir Region in China is an example of an area affected by landslides or related bank destruction.

In the aspects of landslide stability related to hydrological changes, the research is focused on the impact of reservoir or rainfall. Breth (1967) and Muller (1964) analyzed the impacts of reservoir water level changing on landslide stability. Van Asch et al. (1996) analyzed the meteorological and hydrological conditions triggering shallow and deeper landslides in glacio-lacustrine deposits in the French Alps. Deng et al. (2000) and Wu et al. (2001) are interested in the mechanism or stability analysis on the landslide in the reservoir area of the Three Gorges Project, Yangtze River. Chen and Lee (2003) discussed the impacts of the rainfall factors acting on the landslides, presenting a dynamic model for rainfall-induced landslides. Hu (2005), Franco and Claudio (2003) performed the study of the impact of water fluctuation on reservoir landslide stability separately. Panizzo et al. (2005) analyzed the great landslide events in Italian artificial reservoirs in detailed. Goren and Aharonov (2009) examined a thermo-poro-elastic approach on the stability of landslides. Kirschbaum et al.

C. Li · H. Tang (✉) · Y. Ge · X. Hu · L. Wang
Faculty of Engineering, China University of Geosciences
(Wuhan), Wuhan 430074, China
e-mail: tanghm@cug.edu.cn

C. Li
e-mail: lichangdong@cug.edu.cn

Y. Ge
e-mail: cugwgyf@gmial.com

X. Hu
e-mail: huxinli@cug.edu.cn

L. Wang
e-mail: wlq027@126.com

(2009) presented a stochastic methodology to compare the landslide hazard algorithm for rainfall-triggered landslides with an available inventory of global landslide events. Zhang et al. (2010) and Guo et al. (2013) analyzed the hydrological changes in the Yangtze River basin, China.

With respect to the consideration of different influential factors on the stability of landslide, the landslide susceptibility zoning work has inspired many studies at different parts of the world (Vanwesten et al. 2003; Ercanoglu et al. 2004; De Graff et al. 2012; De Graff 1978). Michael-leiba et al. (2003) proposed a GIS-based regional reconnaissance-level assessment of landslide risk to the Cairns community to provide information to the Cairns City Council for planning and emergency management purposes.

It is well known that the reservoir water fluctuation will change the hydrological conditions of the bank slope, which would correspond to increased risk of landslide hazard and bank destruction. The main approaches for bank destruction forecasting are empirical method or statistics method. The first famous empirical formulas was presented by the Kachugin, who proposed the calculation formula of reservoir bank destruction forecasting (Kachugin 1949), and Kondratjev (1956) discussed the influence depth of wave. As for the statistics method, Mosselman et al. (2000) carried out the study on the effect evaluation of bank stabilization on bend scour in Anabranes of Braided Rivers. Malik and Matyja (2008) attempted to reconstruct bank erosion history by examining the anatomical changes in exposed tree roots. Nevertheless, due to the complexity and uncertainty of the landslide bank destruction, there is always a deviation existing between the forecasting results and the actual practice.

In recent years, new technique such as artificial neural and fuzzy inference system networks were employed for developing predictive models to estimate the needed objectives, especially the advantages of neural network began to be recognized. The importance of neural network model applied into landslide susceptibility analyses has inspired many studies, which have tackled the problem from various points of view, especially in the fields of landslide susceptibility assessment and mapping. Ermini et al. (2005), Gómeza and Kavzoglu (2005), Nefeslioglu et al. (2008), Pradhan and Lee (2010), Bui et al. (2012) conducted the landslide susceptibility assessment by utilizing neural network approaches. Furthermore, Lee et al. (2004), Melchiorre et al. (2008), applied neural network method into the landslide susceptibility mapping or zonation. Neaupane and Achet (2004) presented a case study of landslide monitoring and evaluation at Okharpauwa in Nepal by using back-propagation (BP) neural network for landslide monitoring. Sisson et al. (2006) presented an examination of predictive methodologies for the assessment of long-term risks of hydrological hazards, with particular focus on applications to rainfall and flooding, motivated by three data sets from the

Caribbean region. Pozdnoukhov and Kanevski (2008) presented the multi-scale support vector regression algorithm model and to illustrate its use with an application to the mapping of activity given the measurements taken in the region of Briansk following the Chernobyl accident based on data mining and machine learning approach. Mondino et al. (2009) presented a workflow based on neural network algorithms used both for image geometric correction and classification. Yang et al. (2009) investigated the spatio-temporal changes in streamflow of the Guizhou region and their linkage with meteorological influences using the Mann–Kendall trend analysis, singular-spectrum analysis, Lepage test, and flow duration curves. Pradhan et al. (2010) applied a GIS-based BP neural network model in the landslide-susceptibility mapping of Malaysia. Amongst them, the BP neural network is the most popular approach, which is used widely in the engineering practice. However, the neural network is limited to be applied to the field of landslide susceptibility assessment or mapping, and the application of neural network in the field of bank destruction is seldom mentioned. Eroglu et al. (2010) conducted the classifying erosion risks of bare soil areas in the Hatila Valley Natural Protected Area, Turkey utilizing high resolution images and elevation data. Hsu et al. (2011) developed a probability-based methodology to evaluate dam overtopping probability that accounts for the uncertainties arising from wind speed and peak flood. Ding et al. (2013) demonstrated an integrated study by coupling a NPS pollution load estimation sub-model with a distributed hydrological model to simulate the hydrological processes and associated pollution load processes in the Three Gorges Reservoir, China.

Though there are several existing methods of presenting the bank destruction or stochastic approach; unfortunately, few of them are able to take into account the bank destruction study utilizing BP neural network approach based on detailed scenarios. This paper aims to propose a proved effective approach for bank destruction forecasting using BP neural network method based on a detailed case study in the Three Gorges Reservoir Region, China. The above work can lay solid foundation to determine the proper control schemes for reservoir accumulative landslides.

2 Research background

2.1 General introduction

Jinle landslide is one of the typical accumulative landslides in reservoir region, which is situated at Gaoyang Town, Xingshan County, China (Exi Geo-engineering Investigation Institute of HuBei Province 2006; China University of Geosciences 2007). It's at the left bank of Xiangxi River, primary sub-branch of Changjing River, about 30 km

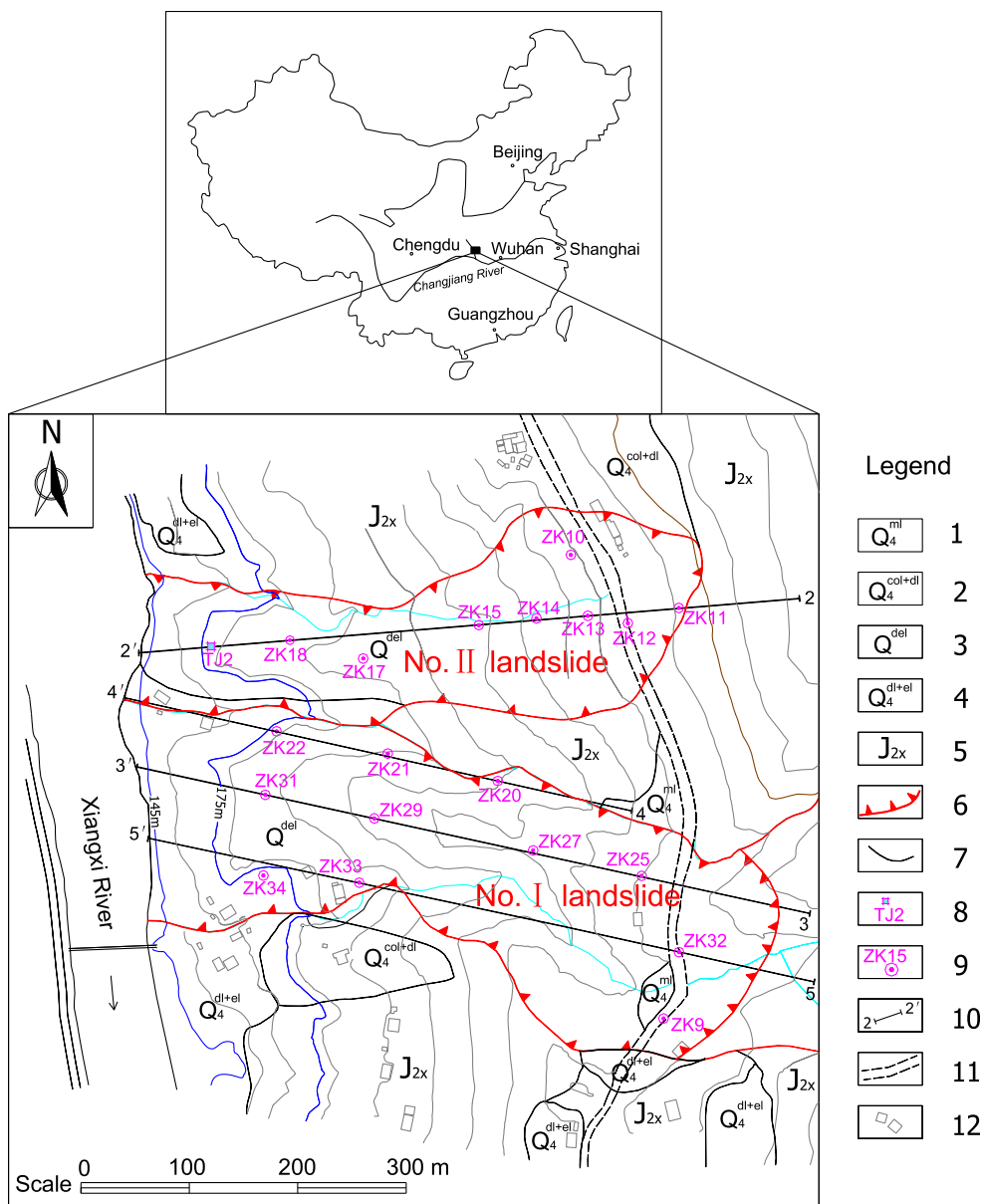


Fig. 1 Engineering geological plane of Jinle landslide. 1 Artificial earth fill; 2 Colluvium and diluvium deposit of Quaternary; 3 Debris of landslide; 4 Eluvium and diluvium deposit of Quaternary; 5

Jurassicstratum; 6 Boundary of landslide; 7 Geological boundary; 8 Test pit; 9 Borehole; 10 Longitude profile; 11 Road; 12 Houses.

upstream distance from the Three Gorges Dam (see Fig. 1). Jinle landslide is composed of two sections, namely No. I landslide and No. II landslide, respectively. The total length of the reservoir bank is about 546 m. These are four long longitude profiles in the research area. Among them, the 2–2' longitude profile in the No. II landslide is selected as the main research object.

2.2 Characteristics of the landslide

The shape of No. II Jinle landslide on the plane is similar to the sole of a shoe. The east–west distance of the landslide

is about 583 m long and 95–217 m in north–south width, with an average width of 140 m. The elevation of the landslide crest is about 330 m. The toe of the landslide reaches the riverbed of Xiangxi River, with an elevation of 140 m (see Fig. 2).

The boreholes exploration can reveal the thickness of the sliding mass, which varies from 6.80 to 23.50 m, with an average thickness of 16.20 m. Generally, the thickness of the sliding mass is large in the front part of landslide and small in the back part of the landslide, which can be clearly shown in Fig. 2. The sliding mass covers an area of $8.16 \times 10^4 \text{ m}^2$, with a volume of $132.22 \times 10^4 \text{ m}^3$.

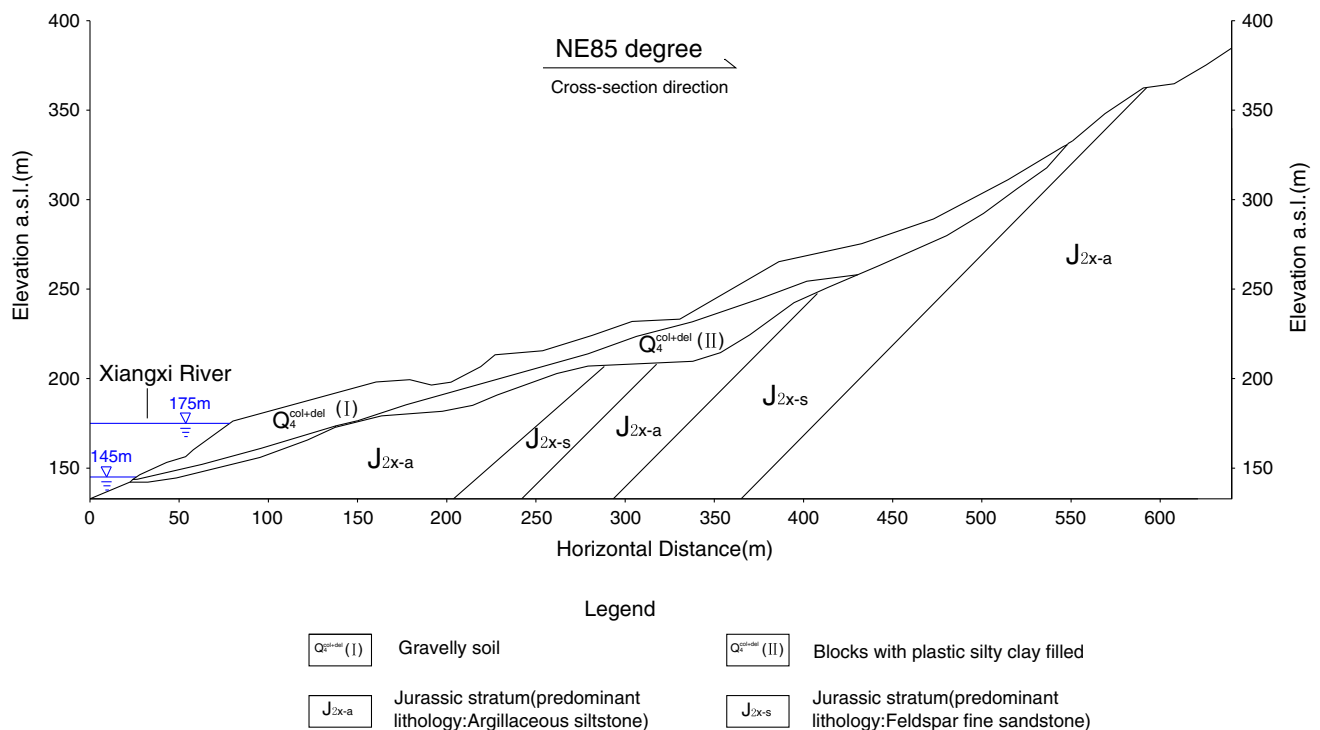


Fig. 2 Typical 2–2 longitude profile of No. II Jinle landslide (Li et al. 2012)

2.3 Substance constituent of landslide

As for the sliding mass, the upper layer substance of the Jinle landslide is composed of grayish and brownish yellow broken and gravelly soil. The underlying layer is the feldspar fine sandstone and a few argillaceous siltstone blocks with plastic silty clay filled, whose block size varies from 2 to 20 cm, angular, with high block content, about 60–80 %.

With respect to the sliding zone, based on the exploration of 10 boreholes and TJ2 test pit, the soil of sliding zone is composed of purplish-red plastic silty clay mixed with gravel, whose gravel content is about 20–30 %; its size varies from 0.2 to 4 cm, subrounded. There is clear slickenside and polish surface in the gravel. The thickness of the sliding zone varies from 0.1 m to 0.8 m.

The sliding bedrock is composed of medium to large thickness layer grayish yellow feldspar fine sandstone and thin to medium-thickness layer purplish red argillaceous siltstone.

2.4 Geo-hydrological condition analysis

There sliding mass is composed of grayish and brownish yellow broken and gravelly soil and rock gravels, with high content of cohesive soil. The components of the gravel are feldspar sandstone and argillaceous siltstone, whose argillaceous content and density will increase after weathering,

which weakens the permeability of the landslide mass. In order to find out the exact permeability coefficient, the water injection test was carried out by Exi Geo-engineering Investigation Institute of HuBei Province (2006).

The main supply of the groundwater in the Jinle landslide area is atmospheric precipitation, where the slope is steep, which is beneficial to centralized drainage of surface water. The groundwater flows from the landslide area towards to the Xiangxi river valley.

3 BP neural network for reservoir bank destruction forecasting

Neural networks may be used as a direct substitute for auto correlation, multivariable regression, linear regression, trigonometric and other statistical analysis and techniques (Singh et al. 2003). A trained neural network can be thought of as an “expert” in the category of information it has been given to analyze. This expert can then be used to provide projections given new situations of interest and answer “what if” questions (Yilmaz and Yuksek 2008). Amongst the traditional neural network methods, BP neural network algorithm is one of the common neural network algorithms which have been widely accepted in many engineering fields. It is constructed by the hierarchy structure, including one input layer, one output layer and one or multiple hidden layers. The node of one layer can only be connected with the nodes of the adjacent

Table 1 Original data sets for neural network analysis

No.	Angle of bank slope (°) X1	Difference of water level (m) X2	Rainfall intensity (mm/h) X3	Particle content (%) X4	Friction angle φ (°) X5	Cohesion C (kPa) X6	Width of bank destruction (m) Y	Remark
1	31.00	12.55	12.00	0.25	33.76	25.44	13.08	China Railway Eryuan Engineering Group Co. LTD (2008)
2	5.00	13.33	12.00	0.35	32.55	23.54	11.82	
3	25.00	21.07	12.00	0.35	33.87	25.12	9.33	
4	18.00	19.67	12.00	0.25	32.43	25.36	3.25	
5	41.00	20.34	12.00	0.25	33.32	23.64	5.57	
6	32.00	20.00	12.00	0.30	32.01	26.71	9.69	
7	29.00	16.27	12.00	0.30	33.66	25.83	12.06	
8	24.00	17.30	12.00	0.30	32.56	23.80	10.27	
9	15.00	33.53	24.00	59.40	32.63	24.42	3.95	Xu et al. (2007)
10	15.00	44.45	36.00	93.71	31.64	22.70	3.30	
11	15.00	63.43	48.00	78.40	33.06	24.04	4.20	
12	25.00	25.43	24.00	93.71	33.47	25.42	84.47	
13	25.00	31.07	12.00	78.40	32.17	25.23	4.60	
14	25.00	61.10	36.00	59.40	34.69	24.61	8.45	
15	40.00	19.66	36.00	78.40	32.61	22.78	54.60	
16	40.00	25.51	48.00	93.71	34.37	24.73	53.35	
17	40.00	36.58	12.00	59.40	32.67	24.94	3.82	
18	55.00	17.16	48.00	59.40	34.16	23.29	46.41	
19	55.00	35.56	24.00	78.40	32.37	25.09	48.30	
20	55.00	53.14	12.00	93.71	32.43	25.00	11.05	

layers. At present, the neural network has been applied to the field of landslide susceptibility assessment or mapping, and the application of neural network in the field of bank destruction could be developed as well.

3.1 Data collection for BP neural network

The data sets for accumulative landslide bank destruction forecasting are sourced from the consultative evaluation reports from the China Railway Eryuan Engineering Group Co. LTD (2008) and the model tests results from Xu et al. (2007). The cohesion and internal friction angles are determined utilizing the approach presented by Lu et al. (2009). The original data sets are listed in Table 1. In this paper, the width of bank destruction is defined by Kachugin (1949) in his paper related to the bank destruction forecasting, in which the width of bank destruction is the horizontal distance from the intersection point of normal high water level and slope surface to the crown of the slope.

3.2 Data preprocessing

It is necessary to conduct the data transformation because of the different magnitude order and units of the six factors, namely X1–X6, which are the angle of bank slope,

difference of water level, rainfall intensity, particle content, friction angle and cohesion, respectively. More and more evidences from the documents and engineering practice show that the scale of bank destruction are significant influenced by the external conditions, such as the change of the water level of river, rainfall intensity, etc. Also, some inherent properties of bank slope including the angle of bank slope, particle content, friction angle and cohesion of soil, should be seriously considered. Therefore, the above external conditions and inherent properties of slopes, including angle of bank slope, difference of water level, rainfall intensity, particle content, friction angle and cohesion, have been widely accepted as the crucial factors influencing the result of bank destruction. Then these six significant factors can be chosen as the main factors adopted in the input layer.

Normalization processing is a good way of obtaining the dimensionless numbers, which can eliminate the unreasonable phenomena so as to improve the accuracy of data processing. The normalization processing could be represented by the Eq. 1.

$$x_{ij}^* = \frac{x_{ij} - \min_{1 \leq j \leq n}(x_{ij})}{\max_{1 \leq j \leq n}(x_{ij}) - \min_{1 \leq j \leq n}(x_{ij})} \quad (1)$$

$(i = 1, 2, \dots, m; j = 1, 2, \dots, n),$

Table 2 Standardized input data for BP neural network

No.	Angle of bank slope (°) X1	Difference of water level (m) X2	Rainfall intensity (mm/h) X3	Particle content (%) X4	Friction angle φ (°) X5	Cohesion C (kPa) X6	Width of bank destruction (m) Y	Remark
1	0.52	0.00	0.00	0.00	0.69	0.68	0.121029	China Railway Eryuan Engineering Group Co. LTD (2008)
2	0.00	0.02	0.00	0.00	0.30	0.21	0.105516	
3	0.40	0.17	0.00	0.00	0.73	0.60	0.074858	
4	0.26	0.14	0.00	0.00	0.26	0.66	0.000000	
5	0.72	0.15	0.00	0.00	0.55	0.23	0.028564	
6	0.54	0.15	0.00	0.00	0.12	1.00	0.079291	
7	0.48	0.07	0.00	0.00	0.66	0.78	0.108471	
8	0.38	0.09	0.00	0.00	0.30	0.27	0.086432	
9	0.20	0.41	0.33	0.63	0.32	0.43	0.008619	Xu et al. (2007)
10	0.20	0.63	0.67	1.00	0.00	0.00	0.000616	
11	0.20	1.00	1.00	0.84	0.46	0.33	0.011697	
12	0.40	0.25	0.33	1.00	0.60	0.68	1.000000	
13	0.40	0.36	0.00	0.84	0.17	0.63	0.016622	
14	0.40	0.95	0.67	0.63	1.00	0.48	0.064024	
15	0.70	0.14	0.67	0.84	0.32	0.02	0.632233	
16	0.70	0.25	1.00	1.00	0.89	0.51	0.616843	
17	0.70	0.47	0.00	0.63	0.34	0.56	0.007018	
18	1.00	0.09	1.00	0.63	0.82	0.15	0.531396	
19	1.00	0.45	0.33	0.84	0.24	0.60	0.554666	
20	1.00	0.80	0.00	1.00	0.26	0.58	0.096035	

where x_{ij}^* is the standardized data; x_{ij} is the original data; min and max are the minimum value and the maximum value in the original data.

The standardized data sets are listed in Table 2.

3.3 Neural network forecasting model for bank destruction

3.3.1 Model establishment

BP neural network can be applied in the field of forecasting the bank destruction, and the corresponding BP neural network graph is shown in Fig. 3.

3.3.2 Parameters setting

The number of the input layer and output layer depend on the practical problem of the application fields. For the forecasting the bank destruction in this paper, there are six elements in the input layer, namely X1–X6, respectively; the output layer only one element, namely Y. However, the number of the hidden layer must be determined by the demands of the users. It is noted that unreasonable element number will cause the increasing of the studying period or more susceptible to errors. Therefore, it is crucial to choose

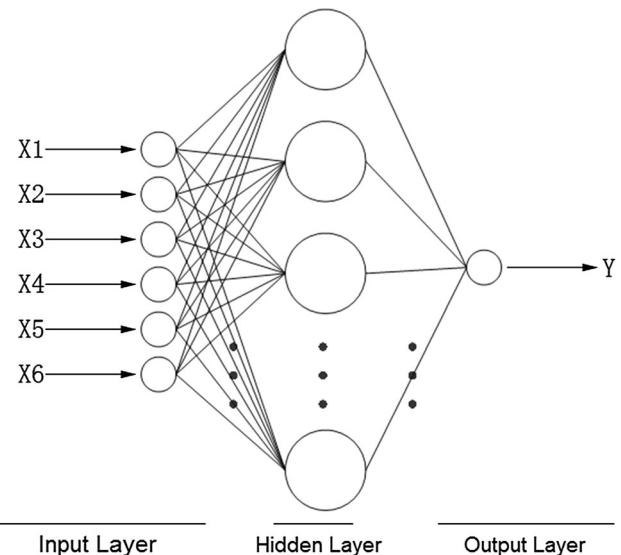


Fig. 3 BP neural network for forecasting the bank destruction

the optimal element number of hidden layer. At present, the optimal element number of hidden layer is often determined by the Kolmogorov’s theory, which can be expressed as follows:

$$m = 2 \times n + 1, \tag{2}$$

where m is the number of the hidden layer, and n is the number of the input layer elements.

For the case study in this paper, there are six input layer elements, i.e., $n = 6$. Hence, m is equal to 13 according to Eq. 2. Due to the setting of the number of the hidden layer elements is relative complicated. Correspondingly, three groups, including $m = 12, 13$ and 14 , are conducted the data training as so to select the best one.

3.3.3 Studying of neural network

The original codes for neural network can be developed to determine the best number of the hidden layer elements.

The training sample in Table 3 are used to conduct the BP neural network simulation under different number of the hidden layer, namely $m = 12, 13$ and 14 . Furthermore, the fitting graph of simulation values and actual values can be represented in Fig. 4 under the error analysis, where the horizontal axis is training data and the vertical axis is the simulation results. The square of coefficient of correlation are 0.9875, 0.9880 and 0.9874 under the $m = 12, 13$ and 14 separately. Therefore, $m = 13$ is best choice because of its lowest error.

Table 3 Cross-reference of simulation results under different number of the hidden layer and actual value

No.	Simulation results			Actual value
	$m = 12$	$m = 13$	$m = 14$	
1	0.216067	0.075108	0.158011	0.121029
2	0.08699	0.056215	0.097115	0.105516
3	0.053772	0.109357	0.002582	0.074858
4	0.04113	0.037989	0.037643	0.000000
5	0.038539	0.025592	0.0618	0.028564
6	0.063722	0.074732	0.074758	0.079291
7	0.042933	0.087927	0.127203	0.108471
8	0.049068	0.098366	0.031381	0.086432
9	0.035101	0.014496	0.030126	0.008619
10	-0.00919	-0.02514	-0.00421	0.000616
11	0.014248	0.019427	0.013469	0.011697
12	0.991343	0.961022	0.995418	1.000000
13	0.009819	0.056346	-0.02473	0.016622
14	0.061138	0.08081	0.058348	0.064024
15	0.620941	0.659205	0.644495	0.632233
16	0.620717	0.620249	0.617965	0.616843
17	0.039292	0.068423	0.030513	0.007018
18	0.526764	0.542451	0.53721	0.531396
19	0.547489	0.535528	0.505267	0.554666
20	0.094763	0.047465	0.139494	0.096035

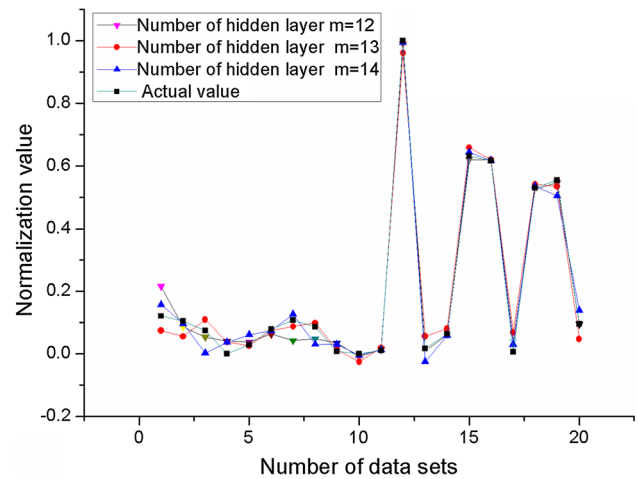


Fig. 4 Comparison among simulation values and actual values

Table 4 Data for bank destruction of Jinle landslide by BP neural network prediction model

Categories of parameters	Value	
	Before normalization	After normalization
Angle of bank slope (°)	36	0.620000
Difference of water level (m)	30	0.342964
Rainfall intensity (mm/h)	54.8	1.188889
Particle content (%)	0.2902	0.000430
Friction angle (°)	33	0.445684
Cohesion (kPa)	24.5	0.449297

4 Forecasting and validation utilizing BP neural network

4.1 Forecasting of bank destruction utilizing BP neural network forecasting model

The forecasting of bank destruction in Jinle landslide can be conducted utilizing the trained BP neural network model. The data for bank destruction of Jinle landslide by BP neural network forecasting model is presented in Table 4. Furthermore, Fig. 5 illustrates that the forecasting presented above has fast convergence and low training error.

The result of above BP neural network program shows that the final width of the bank destruction of Jinle landslide (2–2 cross-section) is 1.4444. The exact width value then can be obtained by Eq. 1 and Table 2, which is equal to 120.56 m.

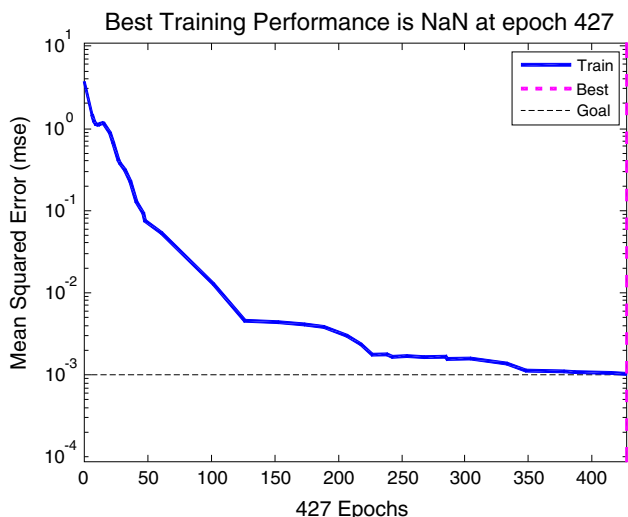


Fig. 5 Training results of BP neural network (training function: trainingdx)

4.2 Validation of bank destruction by independent approaches

In order to validate the affectivity of BP neural network forecasting model in the aspect of bank destruction, two independent approaches, namely empirical method and numerical modeling method, are conducted the bank destruction study separately.

The first approaches for landslide bank destruction forecasting is the empirical formulas for reservoir bank destruction. There are several empirical formulas methods in reservoir bank destruction field. Amongst them, Kachugin (1949) is widely used in the reservoir bank destruction forecasting in China, whose basic calculation model is shown in Fig. 6. The parameters used for reservoir bank

destruction forecasting approach presented by Kachugin (1949) can be obtained from the component of the sliding mass and geometric feature presented in Fig. 2.

The calculation formula of reservoir bank destruction prediction by Kachugin (1949) can be written as follows:

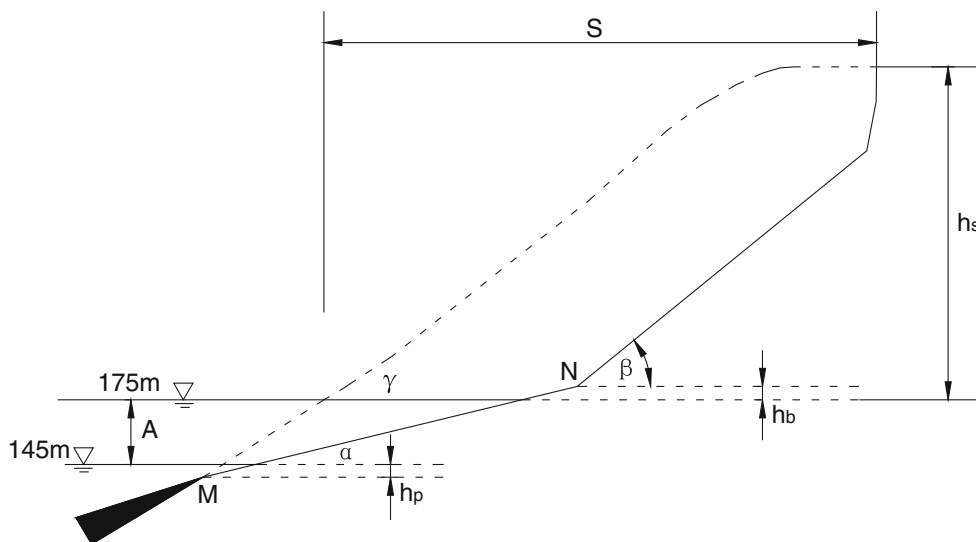
$$S = N \left(\frac{A + h_p + h_b}{\tan \alpha} + \frac{h_s - h_b}{\tan \beta} - \frac{A + h_p}{\tan \gamma} \right), \tag{3}$$

where S is the final width of bank destruction (m); N is a coefficient related to the component of the rock and soil; A is the range of the water fluctuation (m); h_p is the influence depth of wave(m); h_b is the climbing height of the wave (m); h_s is the height of the slope from the normal high water level (m), α is the stable angle of the shoal within the water fluctuation and wave influence range ($^\circ$); β is the stable slope angle above the water level ($^\circ$); γ is the original angle of the bank slope ($^\circ$).

On the basis of the component of the sliding mass, considering the ratio of soil and gravels, the coefficient N should be 0.9, the coefficient α is equal to 13° and the coefficient β is equal to 28° . The water level fluctuates from 175 to 145 m; as a result, the coefficient A is equal to 30 m. The height of the slope at the normal high water level (h_s) and the original angle of the bank slope (γ) can be measured in Fig. 2; therefore, h_s is equal to 25 m and γ should be 30° . On the basis of the site monitoring data related with the maximum instantaneous wind and blowing distance of the wind, the climbing height of the wave (h_b) is equal to 0.84 m and the influence depth of wave (h_p) is equal to 2.00 m by utilizing the empirical equations.

Substitute the above parameters into the classical equations presented by Kachugin (1949), the final width of bank destruction can be calculated, which is 119.03 m (see Fig. 7).

Fig. 6 Prediction method for reservoir bank destruction by Kachugin (1949)



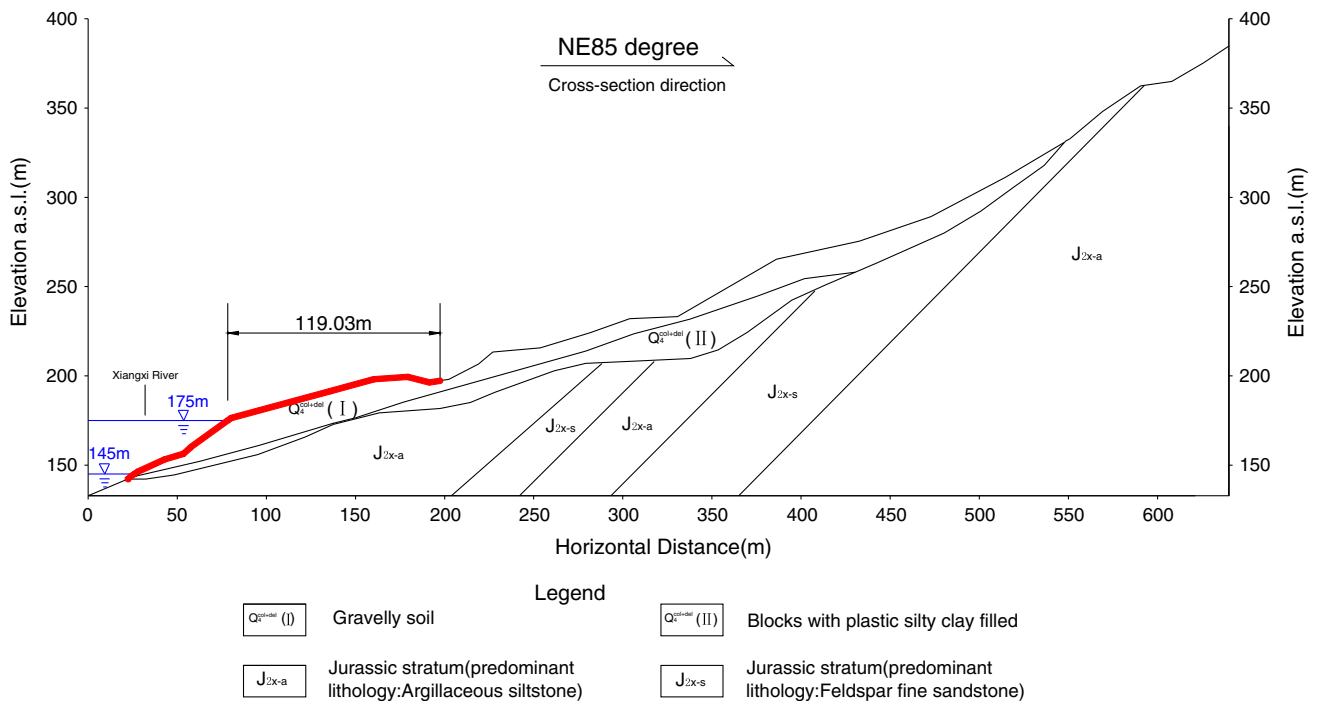


Fig. 7 Reservoir bank destruction forecasting graph of No. II Jinle landslide by empirical method

In order to further validate the effectiveness of the presented bank destruction forecasting approach by BP neural network, another independent approach called numerical modeling can be utilized to conduct the comparison analysis. A typical numerical model set by GeoStudio software can be performed based on the engineering geological model. As a suite of applications for geotechnical and geo-environmental modelling, GeoStudio software includes several modules including SLOPE/W, SEEP/W and SIGMA/W etc., which are widely used in the fields of geotechnical, geo-environmental, civil and mining engineering (Li et al. 2012).

During the numerical modeling on bank destruction forecasting, the SLOPE/W module can be utilized to conduct the slope analysis, the SEEP/W is used to analyze the groundwater seepage and the SIGMA/W is employed to carry out the stress and deformation analysis.

The model adopted by numerical modelling approach is the same with the above model, whose calculation boundary and calculation process can be found in detailed in the paper presented by Li et al. (2012). The searching potential sliding surface obtained from the numerical modeling is shown in Fig. 8. The potential sliding surface in Fig. 8 indicates the scale of reservoir bank destruction. In this numerical model, the final width of bank destruction is 119.71 m.

On the basis of the analysis by utilizing above two independent approaches, namely empirical method and

numerical modeling method, the final width of bank destruction are 119.03 and 119.71 m. The corresponding value we got by the BP neural network forecasting method is 120.56 m (see Fig. 9). Therefore, the percentage error between the forecasting model and the two independent methods are only 1.29 and 0.71 %, respectively, which no doubt validate the high accuracy.

Furthermore, the BP neural network model had obvious advantages over the convention approaches in the aspects of the fast calculation speed and high convenience.

4.3 Bank destruction forecasting for whole landslide

By utilizing the presented new reservoir bank destruction forecasting methods above, the similar steps done in typical 2–2 longitude profile of No. II Jinle landslide can be performed in other cross sections of the reservoir bank. In order to represent the whole bank destruction scale of Jinle landslide region, nine more cross-section are selected to conduct the bank destruction forecasting, namely from 7–7' to 15–15', respectively (see Fig. 10). The corresponding results of the typical cross sections can be obtained in the Table 5.

On the basis of the results of the above sections of the reservoir bank destruction forecasting, the bank destruction forecasting scale in the studying area can be accomplished (see Fig. 10), which can be used as the significant basis for

Fig. 8 Reservoir bank destruction forecasting graph of No. II Jinle landslide by numerical modeling method

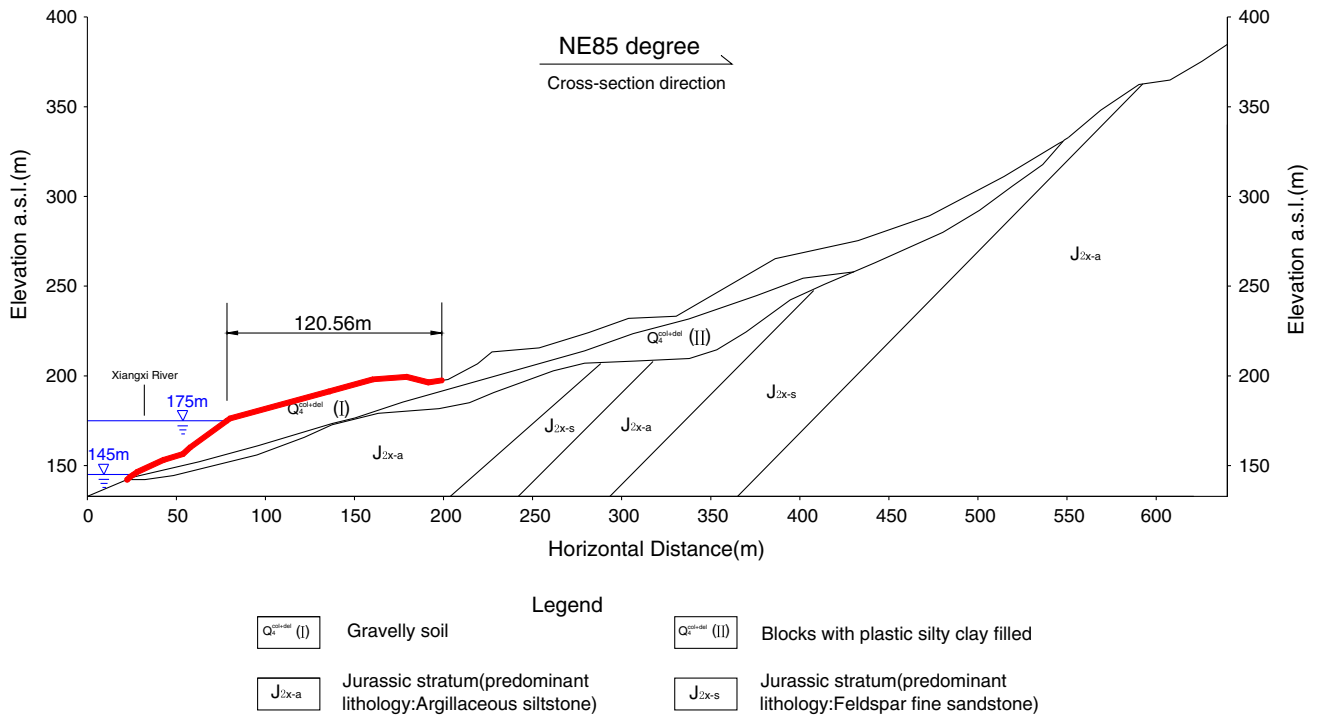
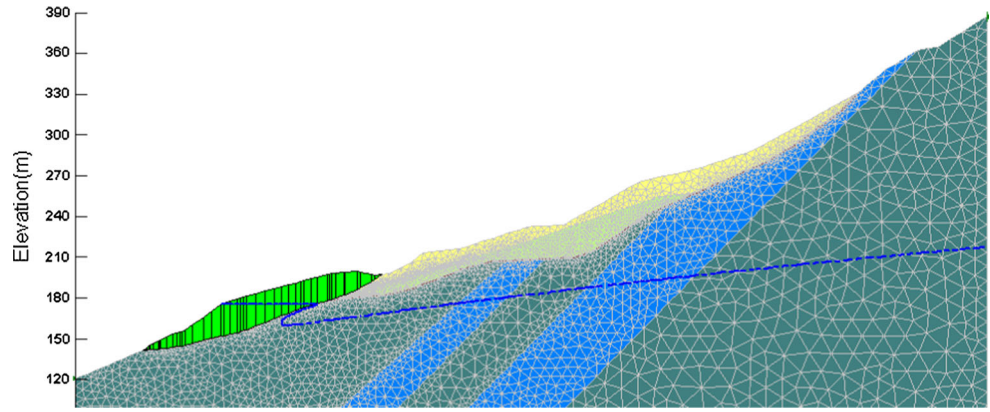


Fig. 9 Reservoir bank destruction forecasting graph of No. II Jinle landslide by BP neural network forecasting method

the protection scheme of Jinle landslide region. The similar accumulative landslides also can be conducted the bank destruction analysis utilizing the presented forecasting model.

According to the bank destruction forecasting scale presented above, the corresponding revetment measures can be proposed to prevent the occurrence of the bank destruction. This recommended control scheme is much more economical scheme than that of the retaining work.

Figure 11 presents a contrast of the Jinle landslide before and after the implement of revetment measure. At present, the control measures of Jinle landslide have been performed over 5 years. During this long period of reservoir water fluctuation, the fact shows that the good

defending effect of the control measures presented above, which can be used as a reference for the similar reservoir landslides in the Three Gorges Reservoir Region.

5 Results analysis and discussion

There are several methods used to conduct the reservoir bank destruction forecasting, but most of them are empirical methods or numerical modeling methods, which need a lot of parameters to draw or calculate the scale of bank destruction. How to get the exact parameters is the crucial and difficult problem for the conventional in the bank destruction forecasting.

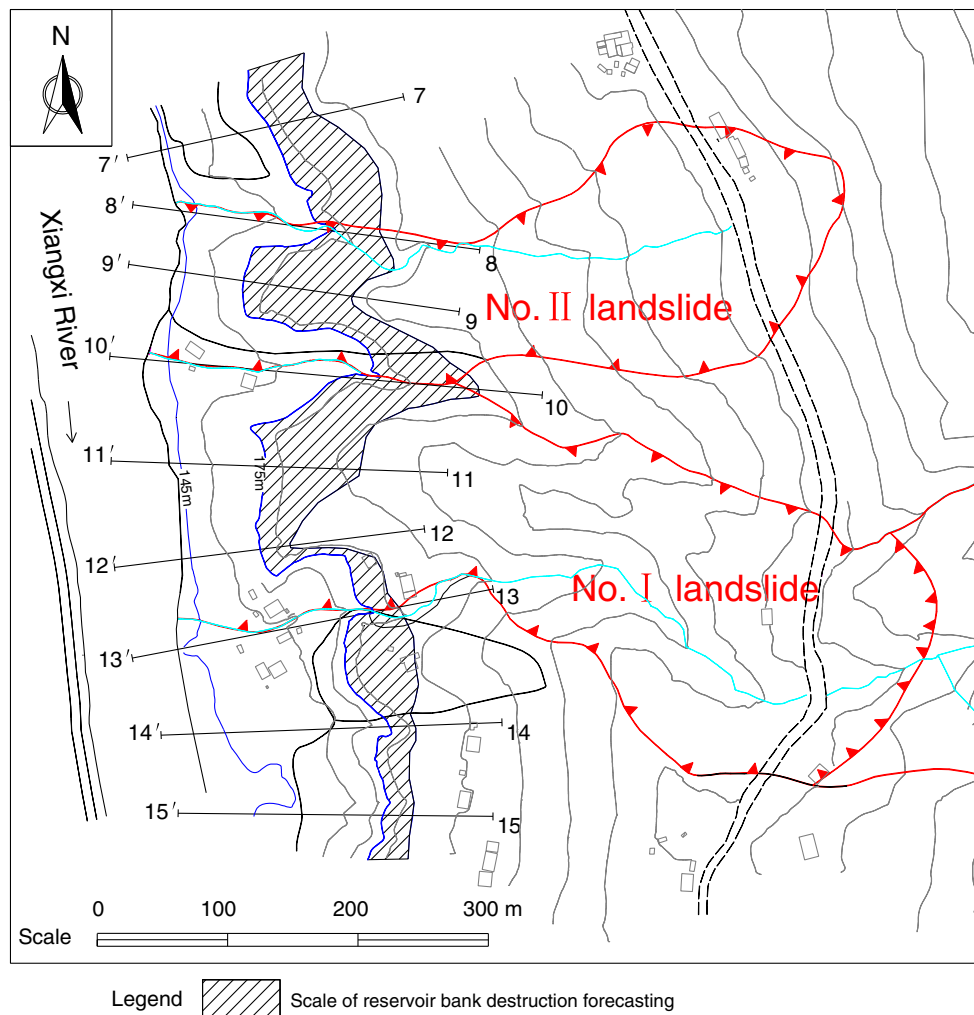


Fig. 10 Bank destruction forecasting planar scale in the whole studying area

Table 5 Bank destruction prediction scale of the whole Jinle landslide region

No. of cross sections	Prediction scale of bank destruction	
	Final width of bank destruction (m)	Highest altitude of bank destruction (m)
7–7'	39.24	191.04
8–8'	36.20	194.47
9–9'	84.38	197.08
10–10'	105.62	193.94
11–11'	73.14	205.17
12–12'	23.30	181.97
13–13'	19.22	180.63
14–14'	19.61	182.15
15–15'	22.52	184.42

The paper conducted the bank destruction forecasting study for accumulative landslides in the Three Gorges Reservoir Region, China utilizing BP neural network

approach, which is much more practical to be applied into the engineering practice. This work can lay solid foundation to determine the proper control schemes for reservoir accumulative landslides.

The bank destruction forecasting scale in the studying area in Fig. 10 is of great importance to the decision-makers, i.e., the bank destruction forecasting scale at least should be covered within the engineering protection, and the corresponding control measures can be put forward against the influences of the adverse factors presented above.

Furthermore, we can clearly find out the shape of the sliding zone of No. II Jinle landslide is the sidestep shape. Once the bank slope is unstable, the retrogressive staged sliding will occur, which will cause the catastrophic sliding of the whole landslide. For the landslide with the similar type sliding zone, it is quite significant to conduct the corresponding optimal reservoir bank defending measures.



Fig. 11 Contrast photos of Jinle landslide before (a) and after (b) the implement of revetment measures

6 Conclusions

Jinle landslide is located at the geological hazards active region, which is under the influence region of the Three Gorges Reservoir. Therefore, it is quite important to discuss the impact of water fluctuation on the stability of bank landslide.

The paper presented a new forecasting model for bank destruction for the accumulative landslides utilizing BP neural network approach. On the basis of the analysis by utilizing two independent approaches, namely empirical method and numerical modeling method, the final width of bank destruction are 119.03 and 119.71 m. The value we got by the BP neural network is 120.56 m. Therefore, the percentage error between the forecasting model and the two independent methods are only 1.29 and 0.71 %, respectively. The results from both the empirical formulas method and the numerical model method well validated the high accuracy of the presented new forecasting model. In addition, the BP neural network model had obvious advantages over the convention approaches in the aspects of the fast calculation speed and high convenience.

The results show that the BP neural network approach is much more practical to be applied into the engineering practice, which can lay solid foundation to determine the scale of bank destruction as well as the corresponding optimal control schemes for reservoir accumulative landslides.

With the results by the bank destruction and corresponding control measures, in the past 4 years, Jinle landslide has been kept in the stable state under long period reservoir water fluctuation. Therefore, the effectiveness of control measures of Jinle landslide has been further validated by the actual engineering practice.

Acknowledgments The work was funded by National Natural Science Foundation of China (Nos. 41202198 and 41230637), the Fundamental Research Funds for the Central Universities (CUG130409 and CUG090104), and National Basic Research Program of China (973 Program) (No. 2011CB710604).

References

- Breth JH (1967) The dynamics of a landslide produced by filling a reservoir. In: 9th International congress on large dams, Istanbul, pp 37–45
- Bui DT, Pradhan B, Lofman O, Revhaug I, Dick OB (2012) Landslide susceptibility assessment in the Hoa Binh province of Vietnam: a comparison of the Levenberg–Marquardt and Bayesian regularized neural networks. *Geomorphology* 171–172:12–29
- Chen H, Lee CF (2003) A dynamic model for rainfall-induced landslides on natural slopes. *Geomorphology* 51(4):269–288
- China University of Geosciences (2007) Control scheme report of Jinle landslide in the Three Gorges Reservoir Region, Xingshan County/ Hubei Province, Wuhan City, China, pp 1–22
- China Railway Eryuan Engineering Group Co. LTD (2008) Documents of geological hazards control consultant department of Three Gorges Reservoir Region, pp 1–10
- De Graff JV (1978) Regional landslide evaluation: two Utah examples. *Environ Geol* 2(4):203–214

- De Graff JV, Romesburg HC, Ahmad R, McCalpin JP (2012) Producing landslide-susceptibility maps for regional planning in data-scarce regions. *Nat Hazards* 64(1):729–749
- Deng QL, Zhu ZY, Cui ZQ (2000) Mass rock creep and landsliding on the Huangtupo slope in the reservoir area of the Three Gorges Project, Yangtze River, China. *Eng Geol* 58(1):67–83
- Ding XY, Zhou HD, Lei XH, Liao WH, Wang YH (2013) Hydrological and associated pollution load simulation and estimation for the Three Gorges Reservoir of China. *Stoch Environ Res Risk Assess* 27(3):617–628
- Ercanoglu M, Gokceoglu C, Van Asch THWJ (2004) Landslide susceptibility zoning North of Yenice (NW Turkey) by multivariate statistical techniques. *Nat Hazards* 32(1):1–23
- Ermini L, Catani F, Casagli N (2005) Artificial Neural Networks applied to landslide susceptibility assessment. *Geomorphology* 66:327–343
- Eroglu H, Cakir G, Sivrikaya F, Akay AE (2010) Using high resolution images and elevation data in classifying erosion risks of bare soil areas in the Hatila Valley Natural Protected Area, Turkey. *Stoch Environ Res Risk Assess* 24(5):699–704
- Exi Geo-engineering Investigation Institute of HuBei Province (2006) Engineering geological investigation report of Jinle landslide in the Three Gorges Reservoir Region, Xingshan County, Hubei Province/Yichang City, Hubei Province, China, pp 19–57
- Franco M, Claudio V (2003) Neotectonics of the Vajont dam site. *Geomorphology* 54(1–2):33–37
- Gómez H, Kavzoglu T (2005) Assessment of shallow landslide susceptibility using artificial neural networks in Jabonosa River Basin, Venezuela. *Eng Geol* 78(1–2):11–27
- Goren L, Aharonov E (2009) On the stability of landslides: a thermo-poro-elastic approach. *Earth Planet Sci Lett* 277(3–4):365–372
- Guo JL, Guo SL, Li Y, Chen H, Li TY (2013) Spatial and temporal variation of extreme precipitation indices in the Yangtze River basin, China. *Stoch Environ Res Risk Assess* 27(2):459–475
- Hsu YC, Tung YK, Kuo JT (2011) Evaluation of dam overtopping probability induced by flood and wind. *Stoch Environ Res Risk Assess* 25(1):35–49
- Hu XL (2005) Numerical simulation on anti-slide construction effects of landslide in Three Gorges Reservoir Region. In Feng CG, Huang P, Ma YE et al. (eds) *The proceeding of the China Association for Science and Technology*, vol 2(1). Science Press & Science Press USA Inc., Beijing, pp 139–143
- Kachugin EG (1949) *The reworking of banks in cases of river affluence*, vol 24. USSR Academy of Sciences Publishers, Moscow
- Kirschbaum DB, Adler R, Hong Y, Lerner-Lam A (2009) Evaluation of a preliminary satellite-based landslide hazard algorithm using global landslide inventories. *Nat Hazards Earth Syst Sci* 9(3):673–686
- Kondratjev NE (1956) Forecast dealing with bank reshaping in the area of water reservoir under the effect of wave action. *Trudy of the State Hydrological Institute*, Issue 56. Hydrometre Publishers, Leningrad
- Lee S, Ryu JH, Won JS, Park HJ (2004) Determination and application of the weights for landslide susceptibility mapping using an artificial neural network. *Eng Geol* 71(3–4):289–302
- Li CD, Hu XL, Tang HM, Fan FS, Wang LQ (2012) Evaluation and control study on reservoir bank landslide in the Three Gorges Reservoir Region, China. *Disaster Adv* 5(4):1501–1507
- Lu XS, Weng XL, Fan WY, SUN XL (2009) The analysis and determination of shear strength of Jinle landslide slip zone. *Coal Geol Explor* 37(4):57–63
- Malik I, Matyja M (2008) Bank erosion history of a mountain stream determined by means of anatomical changes in exposed tree roots over the last 100 years (Bílá Opava River -Czech Republic). *Geomorphology* 98:126–142
- Melchiorre C, Matteucci M, Azzoni A, Zanchi A (2008) Artificial neural networks and cluster analysis in landslide susceptibility zonation. *Geomorphology* 94:379–400
- Michael-leiba M, Baynes F, Scott G, Granger K (2003) Regional landslide risk to the Cairns community. *Nat Hazards* 30(2):233–249
- Mondino EB, Giardino M, Perotti L (2009) A neural network method for analysis of hyperspectral imagery with application to the Cassas landslide (Susa Valley, NW-Italy). *Geomorphology* 110:20–27
- Mosselman E, Shishikura T, Klaassen GJ (2000) Effect of bank stabilization on bend scour in anabranches of braided rivers. *Phys Chem Earth (B)* 25(7–8):699–704
- Muller L (1964) The rock slide in the Vajont Valley. *Rock Mech Eng Geol* 2:148–212
- Neaupane KM, Achet SH (2004) Use of backpropagation neural network for landslide monitoring: a case study in the higher Himalaya. *Eng Geol* 74(3–4):213–226
- Nefeslioglu HA, Gokceoglu C, Sonmez H (2008) An assessment on the use of logistic regression and artificial neural networks with different sampling strategies for the preparation of landslide susceptibility maps. *Eng Geol* 97(3–4):171–191
- Panizzo A, De Girolamo P, Di Risio M, Maistri A, Petaccia A (2005) Great landslide events in Italian artificial reservoir. *Nat Hazards Earth Syst Sci* 5(5):733–740
- Pozdnoukhov A, Kanevski M (2008) Multi-scale support vector algorithms for hot spot detection and modeling. *Stoch Environ Res Risk Assess* 22(5):647–660
- Pradhan B, Lee S (2010) Landslide susceptibility assessment and factor effect analysis: backpropagation artificial neural networks and their comparison with frequency ratio and bivariate logistic regression modeling. *Environ Model Softw* 25(6):747–759
- Pradhan B, Lee S, Buchroithner MF (2010) A GIS-based back-propagation neural network model and its cross-application and validation for landslide susceptibility analyses. *Comput Environ Urban Syst* 34(3):216–235
- Singh TN, Kanchan R, Verma AK, Singh S (2003) An intelligent approach for prediction of triaxial properties using unconfined uniaxial strength. *Min Eng J* 5(4):12–16
- Sisson SA, Pericchi LR, Coles SG (2006) A case for a reassessment of the risks of extreme hydrological hazards in the Caribbean. *Stoch Environ Res Risk Assess* 20(4):296–306
- Van Asch ThWJ, Hendriks MR, Hessel R, Rappange FE (1996) Hydrological triggering conditions of landslides in varved clays in the French Alps. *Eng Geol* 42(4):239–251
- Vanwesten CJ, Rengers N, Soeters R (2003) Use of geomorphological information in indirect landslide susceptibility assessment. *Nat Hazards* 30(3):399–419
- Wu SR, Shi L, Wang RJ, Tan CX, Hu DG, Mei YT, Xu RC (2001) Zonation of the landslide hazards in the fore-reservoir region of the Three Gorges Project on the Yangtze River. *Eng Geol* 59(1–2):51–58
- Xu Q, Bai JG, Tang MG, Huang RQ (2007) Physical modelling for examination of bank collapse in Three Gorges area. *J Eng Geol* 15(2):154–158
- Yang T, Chen X, Xu CY, Zhang ZC (2009) Spatio-temporal changes of hydrological processes and underlying driving forces in Guizhou region, Southwest China. *Stoch Environ Res Risk Assess* 23(8):1071–1087
- Yilmaz I, Yuksek AG (2008) An example of artificial neural network (ANN) application for indirect estimation of rock parameters. *Rock Mech Rock Eng* 41(5):781–795
- Zhang ZX, Tao H, Zhang Q, Zhang JC, Forher N, Hörmann G (2010) Moisture budget variations in the Yangtze River Basin, China, and possible associations with large-scale circulation. *Stoch Environ Res Risk Assess* 24(5):579–589